S.L Rathburn, G.L. Bennett, E.E. Wohl, C. Briles, B. McElroy, and N. Sutfin, 2017, The fate of sediment, wood, and organic carbon eroded during an extreme flood, Colorado Front Range, USA: Geology, doi:10.1130/G38935.1

GSA Data Repository Rathburn et al.

The 2011 DEM was flown on October 25, 2011 by Boulder County at a resolution of 0.75 cm. The 2013 DEM was flown on October 16, 2013 by FEMA at the same resolution. DEM tiles for each year were freely downloaded as grid files from Colorado GeoData Cache and mosaicked in ArcGIS.

TABLE DR1. 2013 FLOOD BUDGET, POST-FLOOD REMOBILIZTION AND LONGER-TERM STORAGE FOR SEDIMENT, WOOD AND CARBON ALONG NORTH ST. VRAIN CREEK, CO

	Location	Process	Sediment (m^3)	Wood (m^3)	Carbon (Mg C)
2013 Input	Hillslope	Landsliding	218,000±66,300	N.D.[*]	2200
	Channel	Bank/bed erosion	289,800±81,400	6200[†]	5100
		Total	507,800±147,700	6200	7300
2013 Output	Reservoir Inlet	Sedimentation	258,200[§]±18,300	4300	1100[#]
	Reservoir Delta	Sedimentation	31,000[**]	N.D.	1700[††]
		Total	289,200±18,300	4300	2800
2013 Storage	Hillslope	Deposition	51,800±6900		
	Channel	Deposition	170,200±73,600	*1900*[§§]	*4500*
		Total	222,000±80,500		
Post-flood Sedimentation	Approach Channel to Delta	Erosion then Deposition	41,000	500	130
Longer-Term Storage	Pre-2013 Reservoir Delta[##]	Sedimentation	16,200	N.D.	5850[***]

[*]N.D. = not determined.

[†]Input of wood calculated based on area of disturbance along trunk channel and tributaries (heavily vegetated pre flood) and an estimated wood volume/ha of 234 m^3/ha from field assessments and remote imagery. Hillslope input of wood is considered negligible as these were not heavily vegetated pre-flood.

[§]A volume of 223,000 m^3 was independently derived from repeat topographic surveys and shallow geophysical surveys (ER and GPR) conducted in spring 2014 before pre- and post-flood lidar were obtained (ER and GPR data in Figure DR8).

[#]Wood as carbon in Mg C is calculated by applying a pine wood volume of 500 kg/m^3 and a 50% wood as carbon value.

[**]Deposition in the delta is based on a post-flood bathymetric survey compared to pre-impoundment topography multiplied by the percentage (65%) of sediment in the delta attributed to the 2013 flood from reservoir core.

[††]Carbon deposited in the delta from average 3% TOC within cored flood sediment in the delta and bulk density of 1.8g/cm^3.

[§§]Quantified as Inputs-Outputs =Storage upstream from the reservoir; listed in italics.

[##]Long-term carbon storage is the pre-2013 flood reservoir delta accumulation estimated from core and TOC analyses.

[***]Storage of pre-flood carbon in the delta using average 20% TOC from pre-flood core and bulk density of 1.8 g/cm^3.

TABLE DR2. RALPH PRICE RESERVOIR SEDIMENTATION RATES FOR THE 2013 FLOOD, POST-FLOOD AND OVER THE 44 YEAR LIFE OF THE DAM.

	Eroded sediment Volume (m^3)	Output sediment volume (m^3)	Sediment Yield ($t/km^2/yr$)*	Lowering Rate (mm/yr)†	Sedimentation Rate (mm/yr)
2013 Flood	507,800	289,200	2125	3.45	420§
Pre-Flood	N.D.#	16,200	2.71	N.D.	5.4**
Post-Flood	N.D.	41,000	300	N.D.	N.D.
Geologic	N.D.	N.D.	N.D.	0.03 – 0.06††	N.D.

*Assumes bulk density of 1.8 g/cm^3. Yield is per event as in 2013 flood.

†Sediment density assumed as 2650 kg/m^3. Lowering rate applies to the 100 km^2 area of LiDAR analysis downstream of Route 7 in which rainfall and flood effects were concentrated (Figure 1).

§Measured in post-flood core collected from reservoir delta. Sedimentation occurred over a 4-day period during the September 2013 flood.

#N.D.=not determined.

**Based on ^{210}Pb analysis of pre-flood sediment collected in core of reservoir delta.

††Measured cosmogenic nuclide erosion rates in the region (Dethier et al., 2014).

TABLE DR3. RALPH PRICE RESERVOIR CARBON LOADING RATES FOR THE 2013 FLOOD, POST-FLOOD AND OVER THE 44 YEAR LIFE OF THE DAM.

	Carbon output (Mg C)	Timescale	Contributing area (km^2)	Carbon yield (Mg C/km^2)
2013 Flood	2800	Event	100	28
Pre-Flood	5850	44 years	265	0.5
Post-Flood	130	1 year	100	1.3

TABLE DR3. TOTAL ORGANIC CARBON (TOC) FOR SEPTEMBER 2013 FLOODING ALONG NORTH ST. VRAIN CREEK, CO COMPARED TO EXTREME EVENTS ON OTHER RIVERS WORLDWIDE.

Location	Drainage Area (km^2)	TOC flux per unit area (Mg C/km^2)	Event recurrence interval (yrs)	Reference
North St. Vrain Creek, CO, USA	100†	28	200	This study
Redwood Creek, N CA, USA	718	28	10	Madej, 2010
Rio Chagres, Panama	414	24	<140	Wohl and Ogden, 2010
Kosnipata Valley, Peru	143	7	26	Clark et al., 2016
Sierra de Las Minas, Guatemala	40-207	160-1520	80	Ramos Scharron et al., 2012
Tsengwen, Taiwan	506	7800±2200	N.A.*	West et al., 2011
Kaoping, Taiwan	3320	4500-9200	N.A.	West et al., 2011
Erlenbach, Switzerland	0.7	585	20	Turowski et al., 2016

*N.A.=not available.

†100 km^2 is the area of LiDAR coverage for this analysis. Overall drainage area is 245 km^2.

Figure DR1. Post-flood wood removal at Ralph Price Reservoir inlet where deposition created an approach channel into the reservoir. View is from west to east looking across the inlet of the reservoir; downstream is to the left in the image.

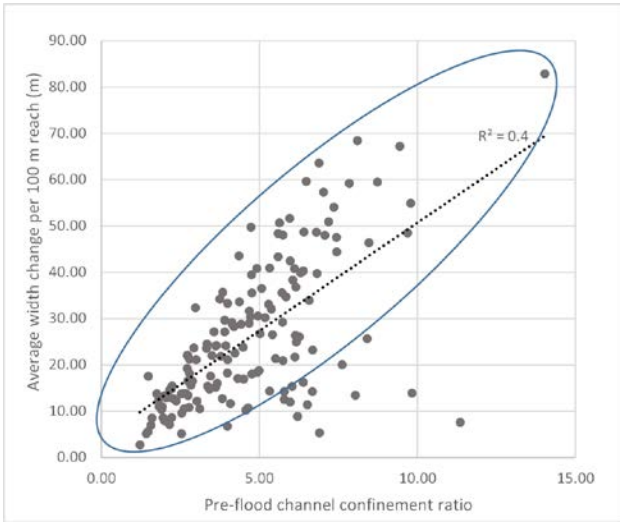

Figure DR2. Channel widening as a function of pre-flood channel confinement ratio, calculated as the ratio of valley width (W_v) to pre-flood channel width (W_c). Pre-flood channel width was mapped from NAIP imagery and valley width was mapped from a combination of NAIP imagery and a pre-flood LiDAR slope map. Channels are considered confined if $W_v \leq 2X\ W_c$, partly confined if W_v 2-8X W_c, and unconfined if $W_v > 8X\ W_c$ (after Wohl et al., 2012). Approximately 90% of the flood channel widening occupied the entire valley floor (points within the blue oval).

A

B

Figure DR3. Flood sediment in storage on the main stem NSV Creek A). View is downstream. B) Flood sediment behind a log jam, main stem NSV, view is upstream with water in a pool shown behind people.

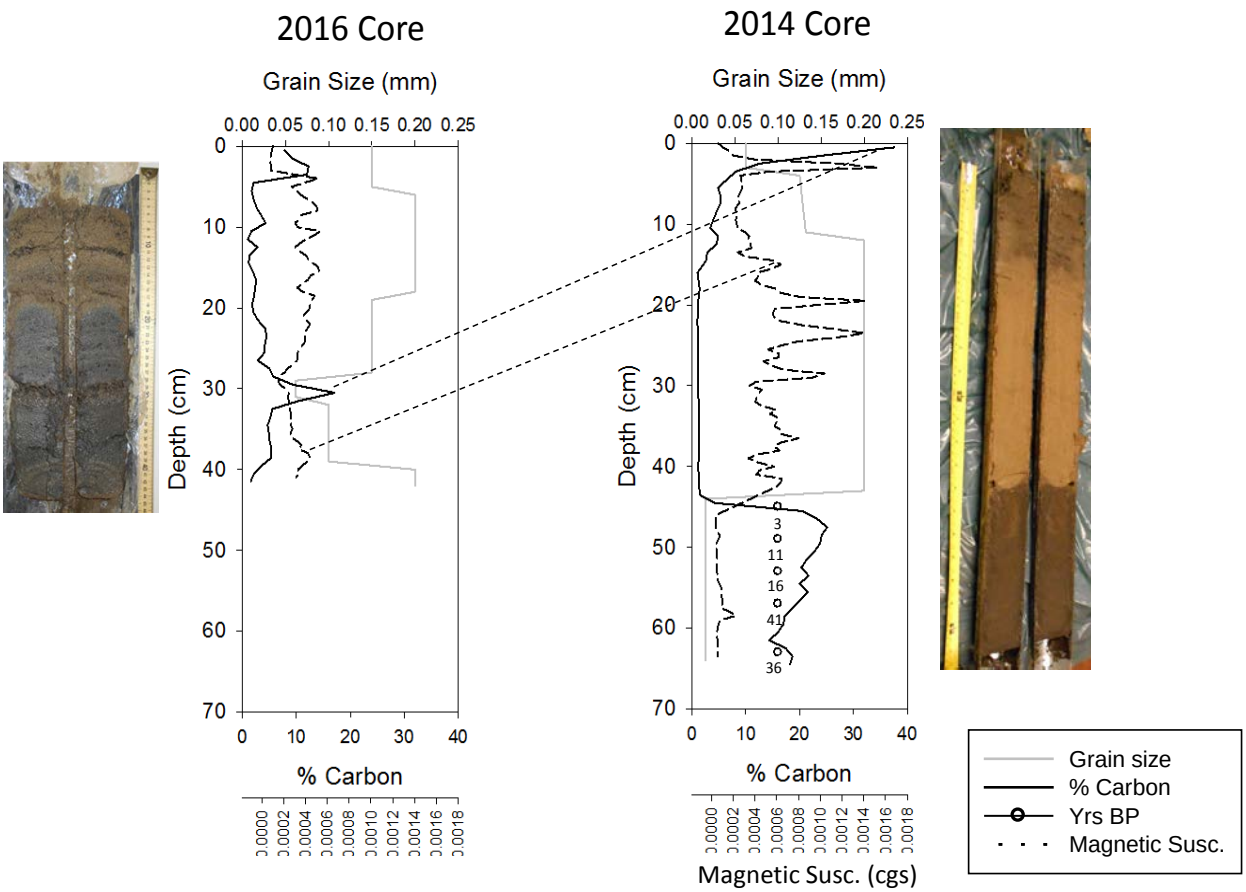

Figure DR4. Reservoir delta core collected in April 2014 and 2016 with grain size, percent carbon as loss-on-ignition, magnetic susceptibility and ^{210}Pb analysis in years BP for the lower sedimentary layers in the 2014 core. Both cores were processed for grain size (bulk composition using gradations of fine-medium sand and silt), percent carbon by loss-on-ignition (LOI) analysis, and magnetic susceptibility. Magnetic susceptibility was measured continuously on the split core using a point sensor Bartington Magnetic Susceptibility Meter MS3 with sub-centimeter resolution. The upper 42 cm of the 2014 core is flood-derived deposition (light colored sand unit), with pre-2013 flood sediments extending from 42 to 64 cm. Correlations as dashed lines between the plots are based on magnetic susceptibility patterns and the presence of a coarse particulate organic rich layer at the top of the 2014 core and at 30 cm on the 2016 core. The upper 30 cm in the 2016 core is interpreted as post-flood sedimentation due to erosion and transport of sediment from the approach channel into the delta as well as erosion of delta sediment followed by deposition farther into the reservoir. The two core locations are 20 m apart as measured along the longitudinal axis of the delta. Compression of the 2016 core occurred as the core barrel encountered consolidated sand from 40-42 cm, limiting core retrieval. Approximately 9 cm and 7 cm of sediment were lost from the core barrel in the 2014 and 2016 samples, respectively. In the 2016 core image, the upper 7 cm are missing due to 1-cm incremental sampling at the field site. Locations of core and samples are as follows: 2014 core N 40^{o} 13.113', W105^{o}23.246'; Eckman dredge sample (not shown on Figure 1) from the middle of the reservoir N40^{o}13.043', W105^{o}22.643'; 2016 core N40^{o}13.118', W105^{o}23.257'.

Delta sedimentation follows the long, narrow geometry of the former channel at the reservoir inlet. Total sediment accumulation at the delta in 2014 was measured at 73 cm; a 64 cm core was collected (Figure 1E), providing a recovery rate of 88%. Core stratigraphy indicates three distinct facies recovered in 2014, including an upper silt and sand recessional flood deposit topped by a visible organic macro layer; a middle, 42 cm thick tan, massive sand flood deposit with an erosional contact into the pre-existing sediment; and a lower (12 cm) organic-rich, silt layer. Analysis of ^{210}Pb of the lower 12 cm of sediment indicates ages of 3 to 41 years BP (prior to the 2013 sampling). The contribution of sediment attributed to the 2013 flood is 65% of the total core length. The remaining 12 cm represents pre-flood deposition since 1969.

We measured $^{210}Pb_{ex}$ and other radionuclides (e.g. ^{226}Ra) by gamma spectrometry in the Dartmouth Short-Lived Radionuclide facility (gamma methods described in more detail in Landis et al. (2012)). $^{210}Pb_{ex}$ is calculated by subtracting ^{226}Ra activity from total measured ^{210}Pb activity ($^{210}Pb_{ex}$=^{210}Pbtotal-minus ^{226}Ra), where ^{226}Ra is the geogenic parent of ^{210}Pb and provides an estimate of ^{210}Pb produced within sediment grains rather than acquired from atmospheric deposition. The error associated with ^{210}Pb analysis ranges from 4-8 years depending on the uncertainty in the initial concentration used in the Constant Initial Concentration (CIC) model, which influences the intercept estimate of the linear regression (interval depth below surface in cm and ^{210}Pb excess in Bq/kg). The CIC model was selected for two reasons: 1) the common Constant Rate of Supply (CRS) model requires recovery of the entire ^{210}Pb profile within the sediment, which was not possible in this case, and 2) the CIC model assumptions are better justified in fluvially-dominated systems where ^{210}Pb is sourced from the surrounding catchment rather than from direct atmospheric deposition to the water body, and the sediment supply is episodic. The age reversal at the bottom of the core is interpreted to indicate sediment contact with a buried profile or analytical error.

A 42 cm core was collected (7 cm lost) in 2016, representing an incomplete sedimentary core because of difficulties probing to the reservoir bottom and hand-driving the Livingston corer through consolidated sandy sediment. Stratigraphy of the core includes an upper silty layer; an organic rich dark sandy layer grading to tan medium sand, and a bottom layer of 2 cm of consolidated sand that fines upward to a coarse organic layer at 30 cm.

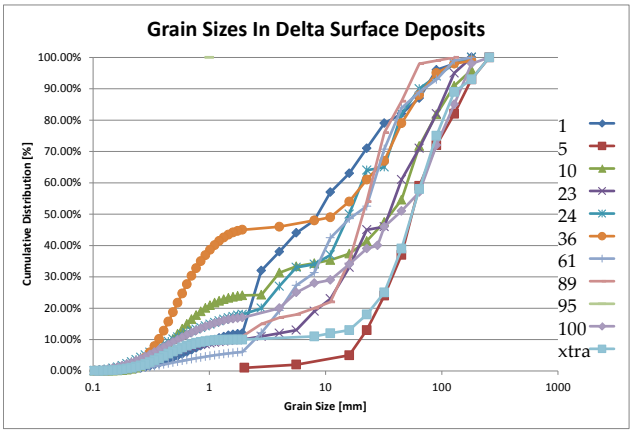

Figure DR5. Cumulative grain size distributions for 2013 flood deposition on the delta surface at 11 randomly selected locations at the inlet and approach channel. D_{50} at the inlet is 9-56 mm or medium to very coarse gravel (average=31mm; coarse gravel). There is a general downstream fining and with distance from the active thalweg of North St. Vrain Creek.

A

B

Figure DR6. Repeat photographs from A) November 20, 2013 and B) October 10, 2015 showing channel incision along NSV Creek at the approach channel that resulted in additional 41,000 m^3 of sediment loading to the reservoir delta during snowmelt in 2014. Bank cut is 3 m high in B). View is downstream towards Ralph Price Reservoir.

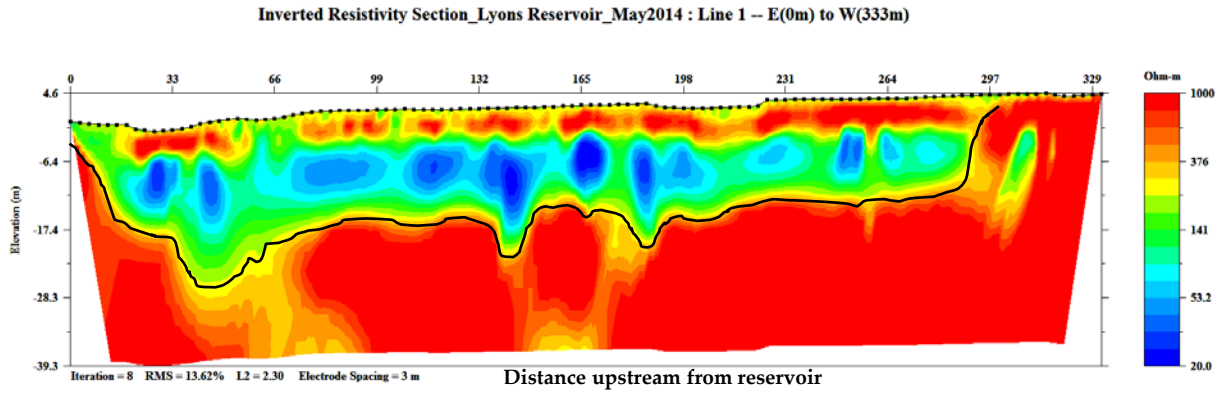

A

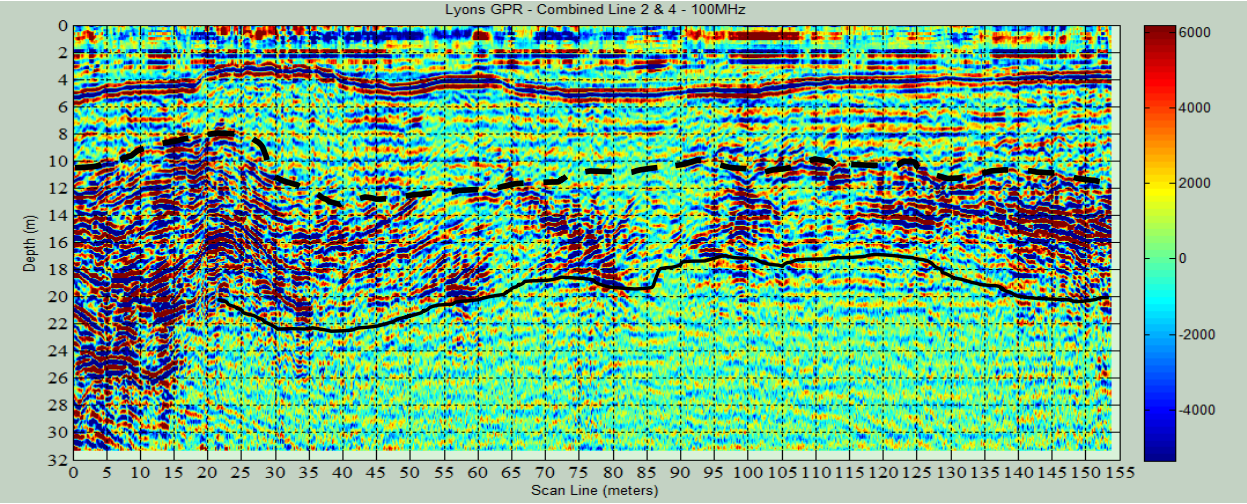

B

Figure DR7. Electrical resistivity (ER; A) and ground penetrating radar (GPR; B) results from a longitudinal survey of the North St. Vrain Creek approach channel into Ralph Price Reservoir. The upper high resistivity layer indicates dry, unconsolidated 2013 flood deposits, overlying a wet, unconsolidated higher porosity and permeability zone. Below the black line is interpreted as the bedrock surface. Horizontal reflections in the GPR indicate dry, unconsolidated sediments above 4 m, with wet, unconsolidated sediment below to the dashed line at 10 m. Irregular reflectors are likely associated with highly unsorted deposits and possibly buried wood at the head of the reservoir delta. The bedrock surface or pre-existing channel bottom is indicated by the sold black line. Both ER and GPR results indicate approximately 18-20 m of deposition above bedrock, which includes pre-flood deposition. Because it is harder to resolve flood from pre-flood sediment using the shallow geophysical surveys, we used the pre- and post-flood airborne LiDAR DoD volumes for the sediment component of the flux graph.

Further support for the high magnitude nature of the 2013 flood is verified by abundant sedimentation within a smaller reservoir downstream from Ralph Price. Longmont Reservoir (1912 masl) was filled completely during the flood, necessitating removal of 56,000 m^3 of sediment during post-flood recovery efforts. This volume is over 4x what has been removed since dredging maintenance began in 1980, with an unknown quantity deposited during a heavy rain storm in May 1995. Importantly, Longmont Reservoir is only 3.2 km downstream distance from Button Rock Dam and has a considerably smaller contributing watershed.

Data Repository References

Clark, K., West, A., Hilton, R., Asner, G., Quesada, C., Silman, M., Saatchi, S., Farfan-Rios, W., Martin, R., Horwath, A., Halladay, K., New, M., and Malhi, Y., 2016, Storm-triggered landslides in the Peruvian Andes and implications for topography, carbon cycles, and biodiversity, Earth Surface Dynamics, v. 4, p. 47-70.

Dethier, D., Ouimet, W., Bierman, P., Rood, D., and Balco, G., 2014, Basins and bedrock: Spatial variation in ^{10}Be erosion rates and increasing relief in the southern Rocky Mountains, USA: Geology, v. 42, p. 167-170, doi:10.1130/G34922.1.

Landis, J., Renshaw, C., and Kaste, J., 2012, Measurement of ^{7}Be in soils and sediments by gamma spectroscopy, Chemical Geology, v. 291, p. 175-185, doi:10.1016/j.chemgeo.2011.10.007.

Madej, M.A., 2010, Redwoods, restoration, and implications for carbon budgets, Geomorphology, v. 116, p. 264-273.

Ramos-Scharron, C., Castellanos, E., and Restrepo, C., 2012, The transfer of modern organic carbon by landslide activity in tropical montane ecosystems, Journal of Geophysical Research, vo. 117, p. 2156-2202, doi:10.1029/2011JG001838.

Turowski, J., Hilton, R., and Sparkes, R., 2016, Decadal carbon discharge by a mountain stream is dominated by coarse organic matter, Geology, v. 44, p. 27-30.

West, A.J., Lin, C.-W., Lin, T.-C., Hilton, R.G., Liu, S.-H., Chang, C.-T., Lin, K.-C., Galy, A., Sparkes, R.B., and Hovius, N., 2011, Mobilization and transport of coarse woody debris to the oceans triggered by an extreme tropical storm, Limnology and Oceanography, v. 56, p. 77-85.

Wohl, E., Dwire, K., Sutfin, N., Polvi, L., and Bazan, R., 2012, Mechanisms of carbon storage in mountainous headwater rivers, Nature Communications, doi:10.1038/ncomms2274.

Wohl, E. and Ogden, F., 2013, Organic carbon export in the form of wood during an extreme tropical storm, Upper Rio Chagres, Panama: Earth Surface Processes and Landforms, v. 38, p. 1047-1416.